

The IMERAPlus Joint Research Project For Determinations Of The Boltzmann Constant

J. Fischer¹, B. Fellmuth¹, C. Gaiser¹, T. Zandt¹, L. Pitre², S. Briau²,
F. Sparasci², D. Truong², Y. Hermier², R. M. Gavioso³, C. Guianvarc'h³,
P. A. Giuliano Albo³, A. Merlone³, F. Moro³, M. de Podesta⁴, G. Sutton⁴,
R. Underwood⁴, G. Machin⁴, D. Del Campo⁵, J. Segovia Puras⁵, D. Vega Maza⁵,
J. Petersen⁶, J. Hald⁶, L. Nielsen⁶, S. Valkiers⁷, B. Darquié⁸, C. Bordé⁸,
C. Chardonnet⁸, C. Daussey⁸, L. Gianfrani⁹, A. Castrillo⁹, P. Laporta¹⁰,
G. Galzerano¹⁰

¹*Physikalisch-Technische Bundesanstalt (PTB), Abbestraße 2-12, 10587 Berlin, Germany*

²*Institut National de Métrologie (LNE-INM/CNAM), 61 rue du Landy, 93210 La Plaine-Saint-Denis, France*

³*Istituto Nazionale di Ricerca Metrologica (INRiM), Strada delle Cacce 91, 10135 Torino, Italy*

⁴*National Physical Laboratory (NPL), Hampton Road, Teddington, TW11 0LW, United Kingdom*

⁵*Centro Espanol de Metrologia (CEM), Alfar 2, 28760 Tres Cantos, Spain and Universidad de Valladolid, Paseo del Cauce 59, 47011 Valladolid, Spain*

⁶*Danish Fundamental Metrology (DFM), Matematiktorvet 30, 2800 Kongens Lyngby, Denmark*

⁷*Institute for Reference Materials and Measurements (IRMM), Retieseweg 111, 2440 Geel, Belgium*

⁸*Laboratoire de Physique des Lasers, UMR 7538 CNRS, Université Paris 13, 99 av. J.-B. Clément, 93430 Villetaneuse, France*

⁹*Seconda Università di Napoli, Via Vivaldi 43, 81100 Caserta, Italy*

¹⁰*Politecnico di Milano and IFN-CNR, Piazza Leonardo da Vinci 32, 20133 Milano, Italy*

Abstract. To provide new determinations of the Boltzmann constant, k , which has been asked for by the International Committee for Weights and Measures concerning preparative steps towards new definitions of the kilogram, the ampere, the kelvin and the mole, an iMERAPlus joint research project has coordinated the European activities in this field. In this major European research project the Boltzmann constant has been determined by various methods to support the new definition of the kelvin. The final results of the project are reviewed in this paper. Determinations of the Boltzmann constant k were achieved within the project by all three envisaged methods: acoustic gas thermometry, Doppler broadening technique, and dielectric constant gas thermometry. The results were exploited by the interdisciplinary Committee on Data for Science and Technology (CODATA) in their 2010 adjustment of recommended values for fundamental constants. As a result, the CODATA group recommended a value for k with a relative standard uncertainty about a factor of two smaller than the previous $u(k)/k$ of 1.7×10^{-6} .

Keywords: fundamental constant, Boltzmann constant, International System of Units, primary thermometry

INTRODUCTION

The General Conference on Weights and Measures (CGPM) agreed at its 24th meeting in October 2011 on new definitions of the kilogram, ampere, kelvin, and mole in terms of fixed numerical values of the Planck constant h , elementary charge e , Boltzmann constant k , and Avogadro constant N_A , respectively. The changes proposed for the International Systems of units (SI) will not actually be adopted until the experimental results on the new definitional constants that are proposed have reached a further stage of refinement. A refined value of the Boltzmann constant proposed for

defining the kelvin would ideally have been determined by at least three fundamentally different methods like acoustic gas thermometry, the Doppler broadening technique, and dielectric constant gas thermometry [1]. These techniques are well beyond the reach of any single national metrology institute, but cooperatively within EURAMET, explored in an iMERAPlus joint research project, the thermometry community developed a coherent set of advanced methods that address this very significant challenge. Accordingly, all determinations of the Boltzmann constant in Europe in the last years were performed and coordinated within the framework of this project.

The paper gives an overview of the achievements during the project duration from 2008 to early 2011.

DIELECTRIC-CONSTANT GAS THERMOMETRY

The basic idea of dielectric-constant gas thermometry (DCGT) is illustrated in Figure 1 and more extensively discussed in [2, 3, 4]. In brief, the density in the well-known state equation of a gas is replaced by the dielectric constant ε and is measured by incorporating a capacitor in the gas bulb. The dielectric constant of an ideal gas is given by the relation $\varepsilon = \varepsilon_0 + \alpha_0 N/V$, where ε_0 is the exactly known electric constant, α_0 is the static electric dipole polarizability of the atoms, and N/V is the number density, i.e. the state equation of an ideal gas can be written in the form $p = kT(\varepsilon - \varepsilon_0)/\alpha_0$. Absolute DCGT requires knowledge of the static electric dipole polarizability α_0 with the necessary accuracy. Nowadays this condition is fulfilled for ^4He . Recent progress has decreased the uncertainty of the ab initio value of α_0 well below one part in 10^6 [5, 6].

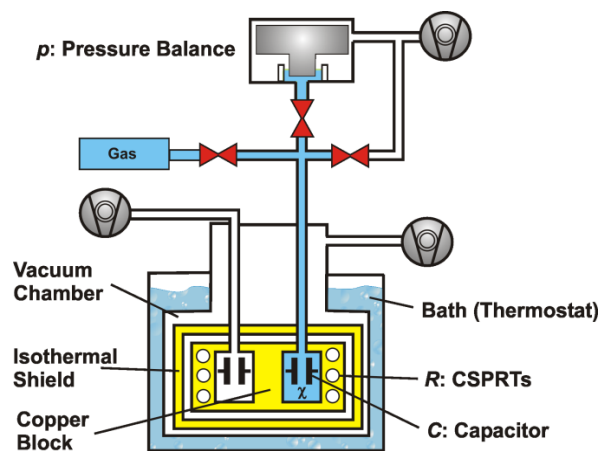


FIGURE 1. Schematic sketch of the DCGT setup used at PTB (reference capacitor on the left, measuring capacitor on the right). Three quantities have to be measured: pressure p , capacitance change $\Delta C/C$ of the measuring capacitor and temperature T via the thermometer resistance R . The CSPRTs (capsule-type standard platinum resistance thermometers) are inserted into holes in the central block or plate made of copper. Three dry pumps are necessary for pumping the two vessels containing the capacitors and the large vacuum chamber, which contains the whole measuring system.

The molar polarizability A_ε is defined as $A_\varepsilon = N_A \alpha_0 / (3\varepsilon_0)$, thus the Boltzmann constant is related to α_0 , A_ε and the gas constant R by

$$k = \frac{R}{A_\varepsilon} \frac{\alpha_0}{3\varepsilon_0} \quad (1)$$

The measurement of the ratio A_ε/R of two macroscopic quantities allows, therefore, the determination of k . For a real gas, the interaction between the particles has to be considered by combining the virial expansions of the state equation and the Clausius-Mossotti equation [3]. For determining A_ε/R , isotherms have to be measured, i.e. the relative change in capacitance $\Delta C/C = (C(p) - C(0))/C(0) = \chi + (\varepsilon/\varepsilon_0) \kappa_{\text{eff}} p$ of the gas-filled capacitor is determined as a function of the pressure p of the gas ($\chi = \varepsilon/\varepsilon_0 - 1$ is the dielectric susceptibility and κ_{eff} is the effective compressibility): The capacitance $C(p)$ of the capacitor is measured with the space between its electrodes filled with the gas at various pressures and with the space evacuated so that $p = 0$ Pa. A polynomial fit to the resulting p versus $\Delta C/C$ data points, together with the knowledge of the pressure dependence of the dimensions of the capacitor (effective compressibility κ_{eff}), yields A_ε/R .

Setup For Measurements At The Triple Point Of Water

The development and the investigation of the components of the setup have been published in different papers, as described below. Here, an overview is given including the results obtained up to now. Isothermal conditions for the measuring and reference capacitors have been realized in a special, large-volume liquid-bath thermostat [7, 8, 9]. Within the working volume of the bath, both temperature instability and inhomogeneity are well below 1 mK. One order of magnitude better are the thermal conditions within the measuring system located in a vacuum chamber inserted in the bath. Thus, the main temperature error is the dynamic temperature-measurement error caused by the gas flow of the measuring gas during the measurement of an isotherm. Dedicated experiments have proven, in accordance with estimations applying the finite-element method (FEM), that the temperature of the capacitor electrodes can be determined with an uncertainty of a few tenth of a millikelvin, which corresponds to a few parts in 10^7 for the determination of the Boltzmann constant.

The extremely sensitive measurement of relative capacitance changes $\Delta C/C$ was performed with a high-resolution and high-precision autotransformer ratio capacitance bridge. A detailed uncertainty budget is presented in [10].

For handling the measuring gas, an ultra-high-purity system using metal gaskets, stainless-steel

tubing and electro-polished internal surfaces was realized. The impurities were analyzed in-situ using a mass spectrometer and an equivalent content of impurities not exceeding the level of one part in 10^6 for k could be verified.

The pressure measurement up to 7 MPa has been performed with the aid of pressure balances designed, constructed and evaluated specifically for the Boltzmann project [11, 12]. Traceability to the SI units has been guaranteed starting from the determination of the dimensions of piston-cylinder systems with the aid of enhanced measurement techniques and performing high-precision cross-float comparisons.

Compressibility And Isotherm Data

The cylindrical capacitors [9] were applied without a cylindrical ground-shield spacer at the top. For determining their effective compressibility resonant ultrasound spectroscopy measurements (RUS) and FEM calculations were performed (for details see [12]). The achieved relative uncertainty amounts to 0.2 %.

A total of eleven isotherms have been measured with helium (nominal purity 99.99999 %, supplier Linde AG) and four with neon (99.9993 %, Linde AG). The isotherms consist of up to fourteen triplets of temperature T , pressure p , and susceptibility χ . The overall number of triplets amounts to 121 for helium and 56 for neon.

For checking purposes, the evaluation of the triplets started with single-isotherm fits, which yielded an optimal order of the fit function of three. For the helium triplets, the resulting fit residuals expressed in terms of pressure are shown in Figure 2.

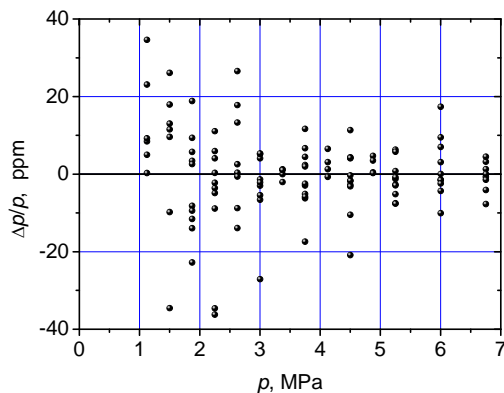


FIGURE 2. Relative single-isotherm fit residuals of all measured helium triplets for the preferred order three of the fit function. Below the preferred pressure range from about 3 MPa to 7 MPa, the scattering is larger due to the small susceptibility of the measuring gas helium.

The final fits were made considering all helium

triplets together performing tests with respect to the statistical significance of the results. The data obtained with neon were used to check the value of the effective compressibility κ_{eff} at an uncertainty level of about 1%.

The complete uncertainty budget for the determination of the Boltzmann constant k by DCGT at the triple point of water (TPW) is given in Table 1. It has been established in accordance with the *Guide to the Expression of Uncertainty in Measurement* (GUM). For the DCGT measurement, the direct access to the relevant uncertainty estimates is hindered because the final result A_{ϵ}/R , yielding k via Equation (1), is gained by fitting. Therefore, the statistical information for estimating the type A components has been deduced by Monte-Carlo simulations. This allows also to consider the pressure dependence of the uncertainty sources. In each case, the simulations have been performed with data sets randomized with the standard deviation of the specific quantity. The type B components are uncertainty sources, which influence the value of k systematically.

TABLE 1. Uncertainty budget for the determination of k by DCGT at the TPW.

Component	$u(k)/k$, ppm
Monte-Carlo simulations (type A)	
Susceptibility (scatter of C bridge)	3.5
Pressure repeatability	1
Temperature instability	0.5
Capacitance instability	5
Type B estimates	
Susceptibility measurement (C change)	1
Determination of κ_{eff} (RUS, FEM)	5.8
Temperature (traceability to the TPW)	0.3
Pressure measurement (7 MPa)	1.9
Head correction (pressure of gas column)	0.2
Impurities (measuring gas)	2.4
Surface layers (impurities)	1
Polarizability ab initio calculation	0.2
Combined standard uncertainty	9.2

Results

The Boltzmann constant has been determined at PTB applying DCGT. In the pressure range from about 1 MPa to 7 MPa, 11 helium isotherms have been measured at the TPW by applying a new special experimental setup consisting of a large-volume thermostat, a vacuum-isolated measuring system, stainless-steel 10 pF cylindrical capacitors, an autotransformer ratio capacitance bridge, a high-purity gas-handling system including a mass spectrometer, and traceably calibrated special pressure balances with piston-cylinder assemblies having effective areas of 2 cm^2 . A value of $k_{\text{TPW}} = 1.380654 \times 10^{-23} \text{ JK}^{-1}$ has been determined for the Boltzmann constant by

performing DCGT measurements at the TPW. Its relative standard uncertainty amounts to 9.2 ppm. Earlier low-temperature DCGT experiments yielded a value of $k_{LT} = 1.380657 \times 10^{-23} \text{ J K}^{-1}$ with an uncertainty of 15.9 ppm [13]. The weighted mean of the two values amounts to $k = 1.380655 \times 10^{-23} \text{ J K}^{-1}$ and has an uncertainty of 7.9 ppm [12].

ACOUSTIC GAS THERMOMETRY

The role of acoustics in a determination of the Boltzmann constant k lies in assuming the validity of the simple proportion between the ideal speed u_0 at which a sound wave propagates in an extremely dilute gas and the mean molecular speed v

$$u_0^2 = \frac{\gamma_0}{3} v^2 \quad (2)$$

where γ_0 is the low density limit of the heat capacity ratio. This assumption enables an acoustic estimate of the mean kinetic energy of a gas of mean molecular mass m at equilibrium near the reference temperature T_{TPW} :

$$mv^2 = 3kT_{TPW} \quad (3)$$

The limit of low pressure is not accessible experimentally, but an experiment which accurately measures the speed of sound u at ordinary pressures may determine k by *estimating* the difference between u and u_0 . This estimate may be made either by extrapolation of a series of measurements at pressures

along an isotherm near T_{TPW} , or by the independent calculation of the non-ideality of the gas.

Among the methods developed for physical acoustics, that employing a steady-state technique via the determination of the resonant frequencies of a cavity of simple and well-defined geometry, is best suited for high accuracy speed of sound measurements in dilute gases. In fact, by 2008 the CODATA value [14] of the Boltzmann constant k was mainly based on the result obtained at the National Institute for Standards and Technology (NIST) in 1988 [15] by measuring the speed of sound in argon at T_{TPW} using a spherical cavity.

Given the sophistication of this experiment and the carefulness with which it had been conducted, it was clear that, to be successful, new acoustic experiments aiming at a determination of k with lower uncertainty would require significant advances in several areas.

In the remainder of this section we review how these activities were successfully developed leading to several acoustic determinations of the Boltzmann constant within the project time scale (Table 2).

All of these results are consistent with the 2008 CODATA [14] value of k . With the exception of the INRiM result which was obtained by measuring the speed of sound in He at a single thermodynamic state, all the other determinations were obtained from the standard practice of extrapolating to estimate the zero pressure speed of sound data in Ar or He measured along an isotherm close to T_{TPW} .

Remarkably, the standard uncertainty associated to the most recent result by LNE-INM/CNAM [19] is a factor of 1.5 smaller than the best previous determination.

TABLE 2. Acoustic determinations of k achieved within project time-scale.

Main Contributor	Gas	Publication, Date	Ref.	k Value \pm Standard Uncertainty, $10^{-23} \text{ J K}^{-1}$	Relative Standard Unc., ppm	Deviation From CODATA 2008, ppm
LNE-INM/CNAM	He	Nov 2009	[16]	$1.380\,649\,5 \pm 0.000\,003\,7$	2.7	-0.7
NPL	Ar	May 2010	[17]	$1.380\,649\,6 \pm 0.000\,004\,3$	3.1	-0.6
INRiM	He	Jun 2010	[18]	$1.380\,640\,4 \pm 0.000\,010\,4$	7.5	-7.3
LNE-INM/CNAM	Ar	Sept 2011	[19]	$1.380\,647\,6 \pm 0.000\,001\,6$	1.2	-2.0

Fabrication Of Resonant Cavities

The advantages of spherical geometry for the determination of the eigenfrequencies of an acoustic resonator had been discussed and verified previously [20]. More recently, quasi-spherical geometries have enabled the use of simultaneous electromagnetic

resonances to determine the thermal expansion of the cavity [21].

At the beginning of the project, the possibility of using microwaves for the absolute determination of the dimensions and shape of a quasi-spherical resonator (QSR) awaited rigorous mathematical proof and experimental verification. As a preparatory step towards the achievement of the latter goal, LNE-INM/CNAM pioneered the realization of copper QSRs advancing state-of-the art design and fabrication

techniques. Some of the cavities realized at this stage were made available by LNE-INM/CNAM to project partners and have been used at NPL [17] and INRiM [22]. The cooperation between NPL and Cranfield University further refined machining and finishing techniques for copper cavities culminating in the realization of an extremely well geometrically defined copper cavity [23] of 62 mm internal radius with measured form errors below 1 μm and surface roughness of a few nanometers (Figure 3). Stainless steel spherical cavities of simpler design were realized and used at INRiM [18] and at CEM/University of Valladolid [24].

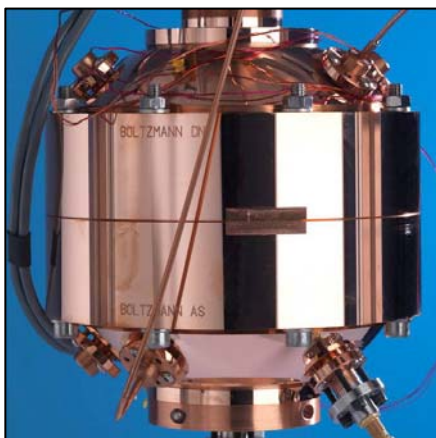


FIGURE 3. Assembled 1-litre volume copper acoustic resonator realized by cooperation of NPL and Cranfield University.

Dimensional Characterization

Significant effort was dedicated to the dimensional characterization of the prototype resonant cavities. Initially, three alternative methods were envisaged as suitable to provide the needed precision and accuracy: water pycnometry; coordinate machine measurements (CMM) and microwave resonances. NPL was the only project partner to pursue all of these three methods. Also, NPL is credited for its main effort in developing and refining the CMM techniques and the mathematical methods for data analysis [23, 25].

Both CMM and microwaves provide information on the cavity dimensions and geometrical shape. While the former information is crucial to convert the measured acoustic frequencies to speed of sound data, the latter is important to make accurate the calculation of geometrical corrections to the experimental microwave and acoustic data. The highest accuracy demonstrated by CMM measurements of the mean radius of a copper ellipsoid was obtained by NPL, with 1.8 ppm relative uncertainty [23]. Comparatively, the reported [23, 18, 19] relative uncertainty of the

microwave determinations of the cavity radius are as low as 0.15 ppm with a corresponding contribution to $u(k)/k$ of 0.3 ppm.

This remarkable advance was made possible by Mehl [26] who published a conjecture for the solution of the perturbation induced onto the electromagnetic field by quasi-spherical geometry. This model was found in outstanding agreement with the experimental observations in several QSRs. These predictions were later confirmed by an even more versatile method worked out at NPL by Edwards and Underwood [27]. Further refinement of the electromagnetic model, keeping into account the relevant perturbing effects of coupling waveguides was worked out by Underwood at NPL [28] leading to the ultimate reduction of the uncertainty related to the microwave determination of the resonator dimensions.

Acoustic Model

For the acoustic part of the experiment, progress was pursued in reducing the influence of several perturbing effects [29]. The predictive capability of the model used to calculate the perturbations induced by geometrical defects was extended beyond the triaxial ellipsoid approximation [30]. Also, dedicated experimental techniques and analytical methods were developed for measuring and modelling: the acoustic impedance of the electroacoustic transducers [31]; the effect of coupling between the acoustic field and the vibrations of the cavity shell [32, 33, 34]; the effects of ducts used for flowing gas through the cavity interior; and the perturbation induced by flow on the acoustic eigenfrequencies [19].

In spite of all these improvements, the uncertainty associated to the determination of the acoustic eigenfrequencies currently limits the ultimate uncertainty achievable in the acoustic determination of k .

Molar Mass

The requirements to prepare and maintain the purity of the gaseous sample used in the experiment reduce the possible choice of the working substance to monoatomic gases. For argon, the required task of assessing the molar mass includes the accurate determination of the isotopic abundances. Within the project, this task has been accomplished by the careful work conducted at IRMM [35]. Gravimetrically traceable synthetic isotopic Ar mixtures were prepared, followed by mass-spectrometric analysis of samples used in the acoustic experiments at NPL and LNE-INM/CNAM. The results obtained at IRMM, having a remarkably low uncertainty ($u_r(M_{\text{Ar}}) =$

0.1 ppm), were later supported by those obtained in an independent determination of the same quantity made at the Korean Research Institute for Standards and Science (KRISS) in cooperation to an experiment for the acoustic determination of k jointly conducted by NIST and the National Institute for Metrology of China (NIM), indicating that the possible variation of the isotopic composition of commercially available Ar samples is rather limited [36].

Acoustic determinations of k using helium have so far been reported by INRiM [18] and LNE-INM/CNAM [16]. The speed of sound in helium being about ten times more sensitive to residual trace impurities than in argon requires a careful assessment of the possible presence of trace impurities. However, the low temperature of the boiling point of helium allows the application of more effective on-site purification procedures, like the use of a liquid helium cold trap.

Extensive work conducted at NPL focused on estimating the effect of outgassing water vapor from the manifold and the cavity comprising the experiment and devised an effective strategy to tackle this problem [37]. Altogether, the purification procedures, the results of the analyses of several commercial samples, and the extensive purging realized by continuously flowing the acoustic experiment allowed to limit the contribution to $u(k)/k$ of the uncertainty associated to the determination of the molar mass below 0.25 ppm in both helium and argon.

Thermometry

Transferring the accuracy achievable in the realization of the triple point of water to the measurement of the temperature of a bulky metallic resonant cavity using capsule-type resistance thermometers is a demanding task and implies the capability to maintain the thermal stability and the temperature uniformity of the experimental apparatus within extremely tight limits. Remarkably, all the research groups involved in the project were able to develop suitable thermostats and calibration/transfer procedures [16–19] which allowed to link the temperature of the acoustic experiments to T_{TPW} with a relative resulting uncertainty $u(k)/k$ below 0.5 ppm, corresponding to approximately 0.15 mK.

DOPPLER BROADENING TECHNIQUE

The Doppler broadening technique (DBT) is a recent method, which has only been explored since 2004. Precision laser spectroscopy of a molecular (or atomic) absorption line in a gas at thermodynamic

equilibrium provides a Doppler broadened profile [38–39, 55, 56] which reflects the Maxwell-Boltzmann velocity distribution of the gas particles (Figure 4). As a result of a highly-accurate analysis of the line profile, taking into account collisional effects (including broadening and narrowing effects), hyperfine structure, saturation of the molecular transition, optical depth, etc, it is possible to retrieve the Doppler width, enabling the determination of k . Three experiments have been developed within the frame of the iMERAPlus project: an Italian setup (involved institutions are: INRiM, University of Naples 2, Polytechnic of Milan) probed initially a CO_2 line at a wavelength of 2 μm and then moved to a water (H_2^{18}O) line at a wavelength of 1.38 μm ; a French setup (involved institutions are: Laboratoire de Physique des Lasers, LNE-INM/CNAM) probes an ammonia ($^{14}\text{NH}_3$) line at a wavelength of 10.3 μm ; and a setup performed by Danish Fundamental Metrology (DFM) probes an acetylene ($^{13}\text{C}_2\text{H}_2$) line at a wavelength of 1.54 μm . In principle this method can be applied to any gas, at any temperature, in any spectral region [57, 58].

Absorption Lineshape

All of these projects require a precise modeling of the line profile, involving common theoretical tools. The absorption lineshape of a single ro-vibrational molecular line is dominated at very low pressure by the inhomogeneous Doppler broadening. In the zero-pressure limit the lineshape is a Gaussian with a half-width Δ_{D} given by:

$$\Delta_{\text{D}} = \nu_0 \sqrt{\frac{2kT}{mc^2}} \quad (4)$$

where ν_0 is the frequency of the absorption line, T is the thermodynamic temperature of the gas, m is the molecular mass and c is the vacuum speed of light. A measurement of the Doppler width Δ_{D} leads to a determination of k . The absorption lineshape is also influenced by a homogeneous collisional broadening (proportional to the gas pressure) leading to an absorption given by a Voigt profile (convolution of a Gaussian and a Lorentzian). At higher pressure, when the molecular mean free path becomes comparable to the optical wavelength, the absorption profile becomes narrower and the lineshape can be described for example by a Galatry or a Nelkin-Ghatak profile (depending on the assumption made for molecular collisions). Other more subtle pressure effects like speed dependent collisions can also be included in the lineshape model to make it even more realistic.

The uncertainty budget associated with the Doppler width measurement is mainly dominated by pressure broadening and various narrowing effects. Indeed one critical part of the DBT is to determine the appropriate physical model to take into account those pressure effects. This point is crucial, as demonstrated by the numerical simulations in Ref. [52, 53]. Several physical lineshape models have been compared, encompassing Gaussian profile, Voigt profile, Galatry profile, Nelkin-Ghatak profile or speed-dependent Voigt profile [46, 48-51, 53].

Laser Spectrometers

The accurate determination of the Doppler widths for NH_3 , H_2O , CO_2 or C_2H_2 molecular lines have required the development of dedicated laser spectrometers [40-45, 54]. Lasers used to probe the molecular gas must exhibit a narrow linewidth, a tunable frequency and a constant intensity (see Figure 4).

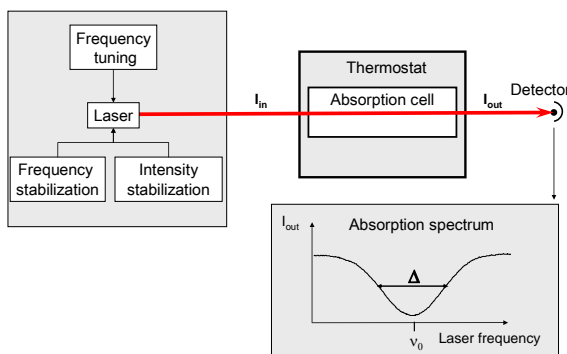


Figure 4. Principle of the Doppler broadening technique.

Both the Danish and Italian experiments use a slave laser, frequency (or phase) locked to a master laser, which is frequency stabilized to the centre of a molecular line using a Doppler free detection. The Danish spectrometer uses a fibre Bragg laser operating at a wavelength of $1.54 \mu\text{m}$ ($^{13}\text{C}_2\text{H}_2$ line) while the Italian one operates with extended-cavity diode lasers at a wavelength of $1.38 \mu\text{m}$ (H_2^{18}O line). They both use an acousto-optic modulator to stabilize the laser intensity at the 10^{-4} level. The French experiment uses a narrow linewidth CO_2 laser at a wavelength of $10.3 \mu\text{m}$ ($^{14}\text{NH}_3$ line). The laser is frequency stabilized onto a molecular line (detected in saturated absorption) and is coupled to an electro-optic modulator which generates two frequency tunable sidebands. A Fabry-Perot resonator is used for the laser intensity stabilization. All the spectrometers demonstrate unprecedented accuracy with ultra low laser intensity

noise (about 10^{-4} at $1.54 \mu\text{m}$ and $1.38 \mu\text{m}$, 10^{-3} at $10.3 \mu\text{m}$), narrow laser linewidth (about 1 kHz at $1.54 \mu\text{m}$, 30 kHz at $1.38 \mu\text{m}$ and 10 Hz at $10.3 \mu\text{m}$), and a broad continuous tuning range of the laser frequency (about 2 GHz at $1.54 \mu\text{m}$, 3 GHz at $1.38 \mu\text{m}$ and 500 MHz at $10.3 \mu\text{m}$).

At low pressure, where all the physical models converge into a simple Voigt Profile, the molecular density and as a consequence the absorption amplitude becomes very small. In this low pressure regime, the signal to noise ratio of the molecular absorption becomes the main limitation of the DBT. To overcome this difficulty, efforts have been made to enhance the signal to noise ratio. As the length of the absorption cell is limited by the thermostat dimensions, multi-pass configurations can be used to enhance the molecular absorption as demonstrated by the French setup [46, 51].

Temperature Control And Traceability

The determination of the Boltzmann constant by the DBT also requires the best achievable control of the gas temperature [46, 47]. In these experiments, it is fixed around 273.16 K, the temperature of the triple point of water where the uncertainty on the measurement of the temperature is the smallest achievable. It is essentially restricted by the application of the (capsule-type) standard platinum resistance thermometers (CSPRT) used to probe the gas cell temperature. Specific thermostats have been developed for the control of the temperature of the molecular gas cell. This kind of thermostat is novel as windows are needed on the absorption cell. The presence of such windows let black-body radiation coming from the laboratory enter the cell. The resulting heat flux produces a thermal gradient along the gas cell.

Two different strategies have been successfully tested by the Italian and French groups. The cylindrical shape of the INRiM thermostat naturally reduces the temperature gradient along the gas cell below 1×10^{-4} K. In this system, the gas cell is included in a temperature controlled thermal shield surrounded by a cooled enclosure under vacuum. As the ensemble operates under vacuum, heat conduction is reduced. Due to its shape and its large heat capacitance, the massive cell ensures thermal equilibrium of the inner gas cell. The length of this thermostat is quite small (about 30 cm) and consequently limits the optical path of the laser beam in the gas. A temperature inhomogeneity and a temperature instability below 1×10^{-4} K have been achieved and maintained for several days.

The French experiment uses a very large thermostat (about 1 m³ of melting ice), which contains an enclosure (vacuum chamber) surrounding itself a thermal shield used to stabilize the temperature of the inner gas cell. With this setup, the gas-cell can be large enough to contain the mirrors needed for a multi-pass configuration. The absorption cell is closed with windows from which pumped buffer pipes extend out of the thermostat walls. For a better control of the thermal gradient along the absorption cell, two iris diaphragms are placed inside the thermostat in order to prevent the infrared laboratory black-body radiation from entering the absorption cell. A temperature inhomogeneity and stability of 3×10⁻⁴ K are achieved with this system.

Uncertainties And Results

The individual uncertainty components in the uncertainty budget have been determined in a collaborative effort by the working group participants. They did share their experience and their results to improve the mathematical treatment of the recorded spectra, which were used to compute the Boltzmann constant. The uncertainty budget has seventeen components among which are lineshape modeling, gas temperature, optical frequency scale, non-linearity of the optical detection, hyperfine structure of the line, optical saturation of the absorption line, gas purity, etc. A global fitting procedure studied and developed by the DFM group has been shared to compare the experimental results of the French and Italian groups. From the Doppler width measurements of NH₃ absorption lines the French group deduced $k = 1.380704 \times 10^{-23} \text{ JK}^{-1}$ with a combined uncertainty of 50 ppm [53]. For CO₂, the Italian group obtained $k = 1.38058 \times 10^{-23} \text{ JK}^{-1}$ with a combined uncertainty of 160 ppm [39, 41]. The best relative uncertainties of type A achieved on the determination of the Boltzmann constant with the DBT is 6.4 ppm with NH₃ [53] and 90 ppm with CO₂ [41].

SUMMARY AND OUTLOOK

Figure 5 shows for comparison a summary of European determinations of the Boltzmann constant since 2007. Motivated by the recommendation of the International Committee for Weights and Measures in 2005, numerous new experiments have subsequently been set up. From measurements with a non-adapted low-temperature version of the dielectric constant gas thermometer (DCGT) of PTB, a preliminary value of the Boltzmann constant was derived with a relative uncertainty of 3×10⁻⁵ [59]. Laboratoire de Physique des Lasers (LPL) undertook a first proof of the

Doppler broadening technique (DBT) with a relative uncertainty of 2×10⁻⁴ [38]. Within the iMERAPlus project the Italian group (UniNA) evaluated the Doppler broadening of a CO₂ line [39, 41]. The acoustic gas thermometry (AGT) measurements of LNE-INM/CNAM [16, 19], NPL [17], and INRiM [18] all used resonators jointly developed within the iMERAPlus project and achieved the smallest uncertainties (listed in table 2) of all methods. LPL evaluated a series of 1420 NH₃ spectra applying a Voigt profile [51], subsequently a Galatry profile [46], and corrected it for the hyperfine structure of the absorption lines [53]. Finally, PTB used DCGT at the TPW [12] with the new thermostat developed jointly with INRiM in the iMERAPlus project.

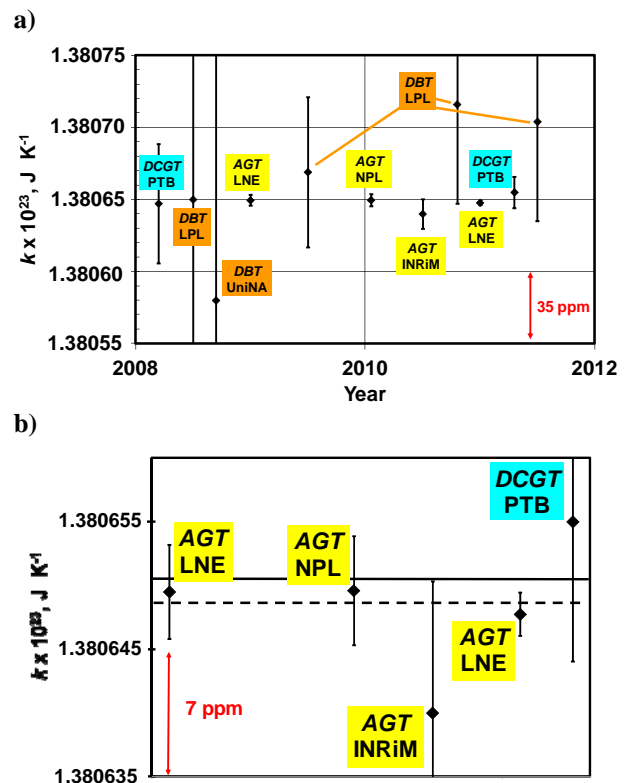


FIGURE 5.

a) European determinations of the Boltzmann constant since 2007. For the abbreviations see text. The error bars denote standard uncertainties.

b) Enlargement of a) depicting the determinations with smallest uncertainties. The full line represents the CODATA value for the Boltzmann constant published in 2008 [14] and the broken line the new value of 2010.

All results are highly consistent and agree very well with the CODATA value of 2008. These new results were recently exploited by CODATA in their 2010 adjustment of recommended values for fundamental constants. As a result, the CODATA

group recommended a value for k with a relative standard uncertainty about a factor of two smaller than the previous $u(k)/k$ of 1.7×10^{-6} . The 2010 value of the CODATA group is shown in figure 5b as well.

For the first determination of the Boltzmann constant by DCGT at the TPW, the two main uncertainty components are connected with the properties of the measuring cylindrical capacitor, namely with its instability and effective compressibility. Progress in decreasing these components significantly is expected by comparing the parameters of capacitors having quite different designs [7], and by using alternative electrode materials, e.g. tungsten carbide, the compressibility of which is smaller than that of stainless steel by a factor of two to three. Considering the experience gained during the first DCGT experiments at the TPW, it seems to be realistic to decrease the relative uncertainty of the Boltzmann constant to a level of only about 2 ppm within one year. Such a result would be the required independent confirmation of AGT [60].

At present, an experiment for the acoustic determination of k by AGT is being concluded at NPL, and experiments will be continued at LNE-INM/CNAM, INRiM and CEM/University of Valladolid. These additional research efforts have a twofold motivation. Firstly, they aim at a further reduction of previously achieved uncertainties by exploiting the improved acoustic features of newly designed cavities. Secondly, the same experiments, with minor modifications, may demonstrate their usefulness for primary and practical thermometry in the near future.

The DBT presents several differences as compared to other better-established methods of primary gas thermometry, besides the basic principles of operation. It can take advantage of recently developed technologies of optical-frequency metrology and, most importantly, a very well defined quantum state is probed. Although the involved molecule may have a natural abundance of other isotopes, only one species is interrogated and the results do not depend on the isotopic composition. The exact modeling of the absorption lineshape is presently the main drawback, but semiclassical models can be successfully employed, provided that the Doppler width is retrieved from an extrapolation to zero pressure with the required uncertainty. Therefore, this method is very complementary to AGT and DCGT.

Accordingly, the CGPM encouraged researchers to continue their efforts and make known to the scientific community in general and to CODATA in particular, the outcome of their work relevant to the determination of k . In addition, the CGPM invited to continue with the preparation of mises en pratique for

the new definitions of the kilogram, ampere, kelvin and mole.

ACKNOWLEDGMENTS

The authors gratefully acknowledge both a personal and a professional debt to Michael Moldover at NIST and Jim Mehl (formerly at NIST and the University of Delaware). The authors are grateful to Wladimir Sabuga and Otto Jusko at PTB who designed, put into operation and characterized the pressure balances. Many other research institutions and private companies have contributed to the project outcome. Special thanks go to: Cranfield University (UK), Université du Maine (F), Scottish Universities Environmental Research Centre (UK), Savimex (F), Rial Vacuum (I), Linde Gas (G), and DH Instruments (USA).

The research within the EURAMET Joint Research Project received funding from the European Community's Seventh Framework Programme, iMERAPlus, under Grant Agreement No 217257 which is gratefully acknowledged.

REFERENCES

1. Fischer, J., et al., *Int. J. Thermophys.* **28**, 1753-1765 (2007).
2. Guggan, D., and Michel, G. W., *Metrologia* **16**, 149-167 (1980).
3. Luther, H., Grohmann, K., and Fellmuth, B., *Metrologia* **33**, 341-352 (1996).
4. Fellmuth, B., Gaiser, Ch., and Fischer, J., *Meas. Sci. Technol.* **17**, R145-R159 (2006).
5. Łach, G., Jeziorski, B., and Szalewicz, K., *Phys. Rev. Lett.* **92**, 233001-4 (2004).
6. Puchalski, M., Jentschura, U. D., and Mohr, P. J., *Phys. Rev. A* **83**, 042508-7 (2011).
7. Zandt, T., Fellmuth, B., Gaiser, C., and Kuhn, A., *Int. J. Thermophys.* **31**, 1371-1385 (2010).
8. Merlone, A., Moro, F., Zandt, T., Gaiser, C., and Fellmuth, B., *Int. J. Thermophys.* **31**, 1386-1395 (2010).
9. Zandt, T., Fellmuth, B., Gaiser, C., Kuhn, A., Merlone, A., Moro, F., and Thiele-Krivoi, B., *Int. J. Thermophys.* **32**, 1355-1365 (2011).
10. Fellmuth, B., Bothe, H., Haft, N., and Melcher, J., *IEEE Trans. Instr. Meas.* **60**, 2522 – 2526 (2011).
11. Sabuga, W., *PTB-Mitteilungen* **121**, 247-255 (2011).
12. Fellmuth, B., Fischer, J., Gaiser, C., Jusko, O., Priuenrom, T., Sabuga, W. and Zandt, T., *Metrologia* **48**, 382-390 (2011).
13. Gaiser, C., and Fellmuth, B., *Metrologia*, **49**, L4-L7 (2012).
14. Mohr, P. J., Taylor, B. N., and Newell, D. B., *Rev. Mod. Phys.* **80**, 633–730 (2008).
15. Moldover, M. R., Trusler, J. P. M., Edwards, T. J., Mehl, J. B., and Davis, R. S., *Phys. Rev. Lett.* **60**, 249–252 (1988).

16. Pitre, L., Guianvarc'h, C., Sparasci, F., Guillou, A., Truong, D., Hermier Y., and Himbert, M. E., *C. Rendus Physique* **10**, 835-848 (2009).
17. Sutton, G., Underwood, R., Pitre, L., de Podesta, M., and Valkiers, S., *Int. J. Thermophys.* **31**, 1310-1346 (2010).
18. Gavioso, R. M., Benedetto, G., Giuliano Albo, P. A., Madonna Ripa, D., Merlone, A., Guianvarc'h, C., Moro, F., and Cuccaro, R., *Metrologia* **47**, 387-409 (2010).
19. Pitre, L., Sparasci, F., Truong, D., Guillou, A., Risegari, L., and Himbert, M. E., *Int. J. Thermophys.* **32**, 1825-1886 (2011).
20. Moldover, M. R., Mehl, J. B., and Greenspan, M., *J. Acoust. Soc. Am.* **79**, 253-272 (1986).
21. Mehl, J. B., Moldover, M. R., and Pitre, L., *Metrologia* **41**, 295-304 (2004).
22. Gavioso, R. M., Benedetto, G., Madonna Ripa, D., Giuliano Albo, P. A., Guianvarc'h, C., Merlone, A., Pitre, L., Truong, D., Moro, F., and Cuccaro, R., *Int. J. Thermophys.* **32**, 1339-1354 (2011).
23. Underwood, R. J., Flack, D. R., Morantz, P., Sutton, G., Shore, P., and de Podesta, M., *Metrologia* **48**, 1-15 (2011).
24. Segovia, J. J., Vega-Maza, D., Martín, M. C., Gómez, E., Tabacaru, C., and del Campo, D., *Int. J. Thermophys.* **31**, 1294-1309 (2010).
25. de Podesta, M., May, E. F., Mehl, J. B., Pitre, L., Gavioso, R. M., Benedetto, G., Giuliano Albo, P. A., Truong, D., and Flack, D., *Metrologia* **47**, 588-604 (2010).
26. Mehl, J. B., *Metrologia* **46**, 554-559 (2009).
27. Edwards, G., and Underwood, R. J., *Metrologia* **48**, 114-122 (2011).
28. Underwood, R. J., Mehl, J. B., Pitre, L., Edwards, G., Sutton, G., and de Podesta, M., *Meas. Sci. Technol.* **21**, 075103 (2010).
29. Guianvarc'h, C., Pitre, L., Bruneau, M., and Bruneau, A.-M., *J. Acoust. Soc. Am.* **125**, 1416-1425 (2009).
30. Mehl, J. B., *Int. J. Thermophys.* **31**, 1259-1272 (2009).
31. Guianvarc'h, C., Gavioso, R. M., Benedetto, G., Pitre, L., and Bruneau, M., *Rev. Sci. Instr.* **80**, 074901 (2009).
32. Pitre, L., Guianvarc'h, C., Sparasci, F., Richard, A., and Truong, D., *Int. J. Thermophys.* **29**, 1730-1739 (2008).
33. Gavioso, R. M., Madonna Ripa, D., Guianvarc'h, C., Benedetto, G., Giuliano Albo, P. A., Cuccaro, R., Pitre, L., and Truong, D., *Int. J. Thermophys.* **31**, 1739-1748 (2010).
34. Truong, D., Sparasci, F., Foltete, E., and Pitre, L., *Int. J. Thermophys.* **32**, 427-440 (2011).
35. Valkiers, S., Vendelbo, D., Berglund, M., and de Podesta, M., *Int. J. Mass Spectr.* **291**, 41-47 (2010).
36. Zhang, J. T., Lin, H., Feng, X. J., Sun, J. P., Gillis, K. A., Moldover, M. R., and Duan, Y. Y., *Int. J. Thermophys.* **32**, 1297-1329 (2011).
37. de Podesta, M., Sutton, G., Underwood, R., Bell, S., Stevens, M., Byrne, T., and Josephs-Franks, P., *Metrologia* **48**, L1-L6 (2011).
38. Daussy, C., Guinet, M., Amy-Klein, A., Djerroud, K., Hermier, Y., Briaudeau, S., Bordé, Ch. J., and Chardonnet, C., *Phys. Rev. Lett.* **98**, 250801 (2007).
39. Casa, G., Castrillo, A., Galzerano, G., Wehr, R., Merlone, A., Di Serafino, D., Laporta P., and Gianfrani, L., *Phys. Rev. Lett.* **100**, 200801 (2008).
40. Galzerano, G., Fasci, E., Castrillo, A., Colluccelli, N., Gianfrani, L., and Laporta, P., *Optics Letters* **34**, 3107-3109 (2009).
41. Castrillo, A., Casa, G., Merlone, A., Galzerano, G., Laporta, P., and Gianfrani, L., *C. Rendus Physique* **10**, 894-906 (2009).
42. Falk, Ch. I., Hald, J., Petersen, J. C., and Lyngsø, J. K., *Applied Optics* **49**, 3854-3859 (2010).
43. Castrillo, A., Fasci, E., Galzerano, G., Casa, G., Laporta, P., and Gianfrani, L., *Opt. Express* **18**, 21851-60 (2010).
44. Hald, J., Nielsen, L., Petersen, J. C., Varming, P., and Pedersen, J. E., *Opt. Express* **19**, 2052-2063 (2011).
45. Galzerano, G., Gambetta, A., Fasci, E., Castrillo, A., Marangoni, M., Laporta, P., and Gianfrani, L., *Applied Physics B* **102**, 725-729 (2011).
46. Lemarchand, C., Djerroud, K., Darquié, B., Lopez, O., Amy-Klein, A., Chardonnet, C., Bordé, Ch. J., Briaudeau, S., and Daussy, C., *Int. J. Thermophys.* **31**, 1347-1359 (2010).
47. Merlone, A., Moro, F., Castrillo, A., and Gianfrani, L., *Int. J. Thermophys.* **10**, 1360-1370 (2010).
48. Casa, G., Wehr, R., Castrillo, A., Fasci, E., and Gianfrani, L., *J. Chemical Physics* **130**, 184306 (2009).
49. Bordé, C. J., *C. Rendus Physique* **10**, 866-882 (2009).
50. De Vizia, M. D., Rohart, F., Castrillo, A., Fasci, E., Moretti, L., and Gianfrani, L., *Phys. Rev. A* **83**, 052506 1-8 (2011).
51. Djerroud, K., Lemarchand, C., Gauguier, A., Daussy, C., Briaudeau, S., Darquié, B., Lopez, O., Amy-Klein, A., Chardonnet, C., and Bordé, C. J., *C. Rendus Physique* **10**, 883-893 (2009).
52. De Vizia, M. D., Moretti, L., Castrillo, A., Fasci, E., and Gianfrani, L., *Mol. Physics* **109**, 2291-2298 (2011).
53. Lemarchand, C., Triki, M., Darquié, B., Bordé, Ch. J., Chardonnet, C., and Daussy, C., *New J. Physics* **13**, 073028 1-22 (2011).
54. Bernard, V., Daussy, Ch., Nogues, G., Constantin, L. F., Durand, P. E., Amy-Klein, A., Van Lerberghe, A., and Chardonnet, Ch., *IEEE J. of Quant. Elec.* **33**, 1282-1287 (1997).
55. Daussy, C., Briaudeau, S., Guinet, M., Amy-Klein, A., Hermier, Y., Bordé, C. J., and Chardonnet, C., *Laser Spectroscopy*, ed. E. Hinds and E. Riis, Singapore: World Scientific, 2005, pp. 104-111.
56. Djerroud, K., Daussy, C., Lopez, O., Amy-Klein, A., Briaudeau, S., Hermier, Y., and Chardonnet, C., *Ann. Phys., Paris* **32**, 175-178 (2007).
57. Truong, G.-W., May, E. F., Stace, M. S., and Luiten, A. N., *Phys. Rev. A* **83**, 033805 (2011).
58. Yamada, K. M. T., Onae, A., Hong, F.-L., Inaba, H., Matsumoto, H., Nakajima, Y., Ito, F. and Shimizu, T. J., *Mol. Spectrosc.* **249**, 95-99 (2008).
59. Gaiser, Ch., Fellmuth, B., and Haft, N., *Talks of the 221st PTB Seminar "Workshop on Progress in Determining the Boltzmann Constant" held on 19th October 2006 in Berlin*, ed. by B. Fellmuth, J. Fischer, Braunschweig: PTB, 2007, PTB-Th-3, pp. 17-25.
60. CCT Recommendation T 2 (2010): Considerations for a new definition of the kelvin, www.bipm.org/utis/common/pdf/CCT25.pdf